Malaya Journal of Matematik, Vol. S, No. 2, 4769-4778, 2020

https://doi.org/10.26637/MJM0S20/1236

Heavy metal Ni removal by activated carbon prepared through the Ionic gelation method

K. Kayalvizhi[1], N. M. I. Alhaji[2], S. Sumera Begam[3] and A. Ayeshamariam[4]

Abstract

The new adsorbent method, the most promising method for treating metal-containing wastewater, and membrane filtration are the most frequently applied methods for treating these complex systems. Meanwhile, the most effective method for treating inorganic pollutants and recovery metals is removing heavy metals with metal concentrations of ¿1000 mg/L. In this study, the limitations of these applications were evaluated reported, and demonstrated that alginate with charcoal beads can be used in treating wastewater contaminated with Ni ions and can be regenerated at least five times before losing their activity. Various physicochemical parameters, such as pH, initial metal ion concentration, and equilibrium contact time, were also studied.

Keywords

Kinetic parameters, nickel, isotherm, activated carbon.

[1,2] *Research Department of Chemistry, Khadir Mohideen College (Affiliated to Bharathidasan University, Thiruchirappalli) Adirampattinam – 614701, Tamil Nadu, India.*

[3,4] *Department of Physics, Khadir Mohideen College (Affiliated to Bharathidasan University, Thiruchirappalli), Adirampattinam – 614701, Tamil Nadu, India.*

[3] *Department of Physics, Bharath Institute for Higher Education and Research, Selaiyur, Chennai-600073, Tamil Nadu, India.*

Article History: Received **01** October **2020**; Accepted **10** December **2020**

©2020 MJM.

Contents

1. Introduction

Numerous chemical-intensive industries discharge large amounts of wastewater containing heavy metals, such as Cd, Cr, Cu, Ni, As, Pb, and Zn, which are extremely hazardous. Sorption involves the transfer of ions from water to soil, that is, from the solution phase to the solid phase. Sorption is actually a series of processes, which include adsorption and precipitation reactions. It is a mass transfer process by which a substance undergoes a mass transfer process by which the substance is transferred from the liquid phase to the surface of a solid and is bound by physical or chemical interactions [1].

Alginate contains 85% of water, which makes it vulnerable to dimensional stability changes. Alginate impressions might undergo a syneresis process, which occurs when water evaporates from an alginate impression after being stored in open air or a high temperature over a certain period. Alginate impression materials are composed of sodium alginate, dehydrated sulfate calcium, potassium sulfate, trisodium phosphate, filler particles, artificial colors, artificial flavors, disinfecting agents, and organic glycol. Good dimensional stability is determined by filler particles in an alginate impression material [2].

Thus, an alginate impression contracts or shrinks and might undergo an imbibition process, by which the alginate impression absorbs water under humid environments or upon exposure to water. The process causes the expansion of the material. Dimensional stability changes can occur because of either syneresis or imbibition processes [3]. The steps for alginate impression include rinsing the impression under running water, spraying with disinfection solution, covering with damp cloth before inserting it in a sealed bag for the maintenance of alginate dimensional stability, and lastly pouring the impression with cast materials. The steps require the monitoring of alginate impression storage and preventing dimensional stability change. Moisture in the alginate impression must be ensured for the maintenance of the dimensional stability of the impression. The storage of the impression can be covered with a damp cloth or placed in a sealed bag. In this research, seal bag was used as a storage material for the alginate mold because it is effective and easy to handle. The pouring of an impression is often delayed because of time limitation [4].

High-precision alginate is used as an impression for chromatic phase indicator infection control and disposable products line used in dentistry. Alginate is used in dental applications requiring low accuracy. Several faults can be encountered when using an alginate impression material but can be generally be prevented through adequate mixing, correct spatulation, correct storage of the set material, and the timely pouring of the impression. Owing to the increased accuracy of elastomers, secondary impressions using these materials are often preferred over alginate. Patients prefer the overall experience of having an impression taken with an elastomer over using alginate and prefer resultant dentures [5].

Catalysis is an extremely important branch of science and is vital to our modern society. The preparation of approximately 90% of all processed chemical compounds involves the use of catalysts at some stages of their production. In general, catalytic reactions are more energy efficient than other process, and reduces waste and undesirable compounds, at least in the case of highly selective reactions. These features are important considerations when addressing the dwindling global reserves of raw materials, such as activated carbon.

The special nature of carbon, combined with the molecular perfection of single-walled nanotubes, endow the nanotubes with exceptional material properties, such as extremely high electrical and thermal conductivity, strength, stiffness, and toughness. No other element in the periodic table bonds to itself in an extended network and has a strength comparable to that of a carbon–carbon bond. The delocalized pi-electron donated by each atom is free to move in the entire structure, rather than remaining with its donor atom, and thus gave rise to the first known molecule with metallic type of electrical conductivity. Furthermore, high-frequency carbon–carbon bond vibrations provide an intrinsic thermal conductivity that is higher than that of other materials, even diamond. However, in most conventional materials, actual observed material properties: strength and electrical conductivity are substantially degraded because of the occurrence of defects in their structures. Activated carbon, achieve values that are extremely close to their theoretical limits because of the molecular perfection of its structure; thus, we selected activated carbon as an adsorbent [6].

Activated carbon that is less than 100 nanometers in diameter can be manipulated chemically and physically in useful ways. It has an incredible range of applications in material science, electronics, chemical processing, energy management, and many other fields. Activated pure carbon can be manipulated using the well-known and the tremendously rich chemistry of carbon. This provides opportunity for modifying its structure and optimizing its solubility and dispersion. Activated carbon is molecularly perfect, that is, it is normally free of property-degrading flaws in its nanostructures. These extraordinary characteristics account for the potential applications of activated carbon [7].

Active carbon with randomly arranged microcrystallites and strong cross-linking has a well developed porous structure, which forms during the carbonization and activation processes when the space between elementary crystallites are cleared of tar and other carbonaceous material. The activation process enhances the volumes and enlarges the diameters of the pores. The structures of the pores and their size distribution are largely determined by the nature of a raw material [8].

Park H.G et al., reported that, by combining two functions of alginate gel and activated carbon, an activated carbon-containing alginate bead (AC-AB) adsorbent was developed and successfully used in simultaneously removing heavy metal ions and toxic organics. Quantitative analysis showed that the adsorption of almost all toxic organics, such as p-toluic acid is caused by activated carbon in the AC-AB adsorbent and the alginate component has a major role in the removal of heavy metals. A 50 L solution containing eight heavy metals (Pb^{2+}, Mn^{2+}, Cd^{2+}, Cu^{2+}, Zn^{2+}, Fe^{2+}, Al^{3+}, and Hg^{2+}) and four mineral ions was run continuously through a filter cartridge packed with 160 g of the AC-AB adsorbent. In this report, the adsorbent showed a high capacity to remove heavy metals completely from water while allowing essential minerals, such as K^{+}, Na^{+}, Mg^{2+}, and Ca^{2+}, to pass through the filter. The adsorbent was regenerated using elements, such as HNO3, and reused repeatedly up to 10 cycles of adsorption and desorption without showing considerable loss in its metal uptake capacity. The AC-AB adsorbent had enormous potential as a drinking water treatment technology owing to its high capacity and high selectivity for toxic heavy metals [9].

Idris, A et al. successfully synthesized magnetic alginate beads by incorporating ferrofluids based on maghemite nanoparticles (γ-Fe_2O_3) and sodium alginate, with the size of uncoated and citrate coated γ-Fe_2O_3 to be 15 nm and 9 *nm* respectively. The specific saturation magnetization (σ_s) value of coated particles was lower than that of uncoated particles. The zero coercivity of the magnetization curve indicated that the particles were super paramagnetic in nature. Ferrofluids and alginate solution magnetic beads in a ratio of 1:10 were

prepared, and the ability of magnetic beads to remove Pb(II) ion from aqueous solutions in batch media was investigated. The results revealed that 95.2% of the Pb(II) was removed within 2 h at pH 7. The equilibrium amount of Pb(II) adsorbed onto the magnetic beads approached a constant value with increasing concentrations, suggesting that the uptake of Pb(II) followed a Langmuir-type adsorption equation at a qmax of 50 mg/g. For determining the reusability potential of an adsorbent, isolated beads can be used as regenerated sorbents in repeated sorption–desorption cycles, and these magnetic beads can be used in treating wastewater contaminated with heavy metals [10].

2. Experimental

The methods of Alginate gel preparation can be loosely divided into four groups: solvent evaporation, neutralization, cross-linking, and ionotropic gelation methods. The ionic gelation method is mainly used in preparoffing the spherical beads varying in size and porosity. The process involves the dropwise addition of an alginate gel solution, followed by cross-linking. Enzymes may be immobilized on the beads by adsorption or covalent binding to the matrix. Calcium chloride is usually used as a cross-linking and activating agent because of its bifunctionality, reliability, and easy use. The model proteolytic enzyme selected for immobilization in this study was trypsin because of its high efficiency, specificity, and wide use in biotechnology and medicine [11].

Alginate (0.2 g) and charcoal (0.6 g) were dissolved in 10 mL of 2% (w/v) acetic acid under mild stirring overnight. The system used for the production of alginate with charcoal beads was added dropwise through a flat-tip needle with an internal diameter of 0.31 mm (flow rate = 0.3 mL/min) to a calcium chloride (10% w/v) solution under stirring. Given that alginate is insoluble at a high pH, the drops solidified because of polymer precipitation. The obtained beads were filtered and washed with distilled water for the removal of residual calcium chloride and stored in water. Exactly 1.5 g of swollen beads were suspended in 25 mL aqueous solutions under mild magnetic stirring. Calcium chloride reacts with the primary amine groups of alginate with charcoal. Thus, calcium chloride with a molar ratio of (1:1) was studied upon exposure to the beads for 4 h at 20°C under mild stirring. Alginate with charcoal beads was then washed with distilled water for the removal of residual chloride ions and stored in water. The solution was filtered and dried under room condition after drying get in an air-tight container [12].

A 0.01 M $NiSO_4$ solution was prepared for the preparation of a stock solution from the stock solution of 0.005 M NiSO4 solution and used in the analysis of the adsorption capacity of activated carbon alginate beads. A 0.005 M NiSO4 solution was used at various concentrations (ppm), then 0.1 mg of alginate beads were added after the equilibrium time of the solution was achieved. Afterward, coloring agents were added (bromine water + dimethyl glyoxime) the concentration were measured by using UV Spectrometer Photometer at 440 nm. HCl4 was used to study the variation of pH of the experiment [13].

2.1 UV-Absorption Method

A standard stock solution of copper was prepared at 600 ppm by using $NiSO_4$. Different initial concentrations of Ni solution were prepared from stock solution, and the absorbance of the Cu solution was used in preparing a standard graph through the UV spectrophotometric method. Excactly10 mL of the solution was kept in a stirrer for 120 min after the addition of 100 mg of adsorbent. Then, 5 mL of the solution was mixed with 10 mL of SMF, and 2 mL of $K4[Fe(CN)_6]$ was added until a final volume of 10 mL. The absorbance of the solution was measured, and the concentration of Ni after adsorption was calculated from the standard graph [14].

2.2 Calorimetric Method

Optimum concentration was determined after the experimental studies at various initial metal ion concentrations ranging from 20 and 120 ppm. Adsorption capacity was increased by increasing the initial metal ion concentration at a certain level. After the saturation of the metal ion, no change was observed on the surfaces of pores. The minimum percentage uptake of Ni ion was observed at low concentrations and increased with initial concentration. At the saturation level (120 ppm), the uptake of Ni ion decreased because of the lack of adsorption sites on activated carbon prepared using alginate with a charcoal surface [15].

From the stock solution, different concentrations of the Cu solution were prepared, then 0.1 g of the adsorbent was added. Before and after adsorption, the concentration of Cu was estimated by using a (model) UV-VIS spectrometer. Experiments were performed using different concentrations of the adsorbent adsorbate, times, pH values, and agitation speed. Adsorption capacity was calculated by using the following formula [1]:

$$Q_6 = \left[\frac{(C_0 - C_6)}{W} V\right]$$

C_0 = Initial concentration of Ni ion(ppm)
C_e = Final concentration of Ni ion
V = volume of Ni ion solution (mL)
W = weight of the adsorbent alginate with charcoal acting as activated carbon (g)

2.3 Characterization

XRD powder diffractions were acquired using a Simiens D5005 diffractometer with Cu Kα radiation source. The samples were recorded at of 2θ of 5°–80°, with a step of 0.02°. FTIR measurements were performed for the identification of functional groups present in the adsorbent with a Perkin Elmer dual frontier equipped with a diffuse reflectance infrared Furrier transformed (DRIFT) collector accessory at a resolution of 4 cm^{-1} and 128 scans. The surface morphology was investigated by SEM in a JEOL microscopy, model JSM-7500F. An electron beam with an acceleration voltage of 2 kV

was used. The software Image J (version 1.45s) was used for image treatment. The samples were dispersed in isopropanol and deposited in a silicon grid before.

3. Results and discussion

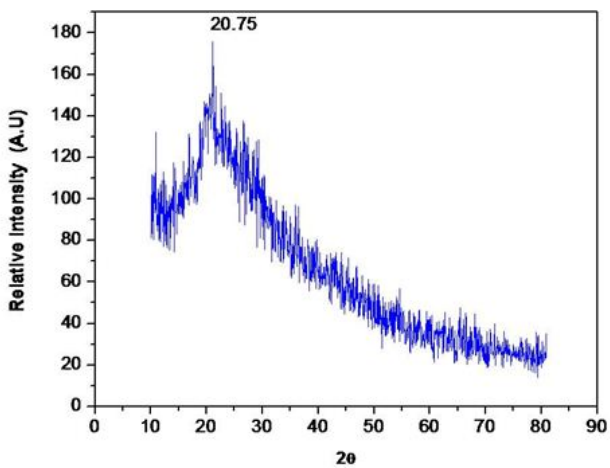

Figure 1. XRD analysis of the activated carbon adsorbent prepared using alginate with charcoal

The peaks at 2θ of 20.75° corresponds to the (220) reflections of activated carbon, indicating the presence of randomly oriented crystallites. Its value matches that of JCPDS-82-0505 and has a cubic structure and a lattice constant 14.26. No characteristic peaks of impurity and other phases were observed. The intensity of (220) plane becomes progressively dominant, and the (220) axis represents the formation of a single crystal with a cubic structure. Moreover, with increasing temperature, the full width at half maximum (FWHM) of (220) plane decreases, indicating improvement in the structural order of activated carbon. The observed relationship between the degrees of (220) preferred orientation may be explained in terms of the migration of molecules onto the growing surface. The crystallite size 'D' of activated carbon was calculated by using Scherrer's formula [16]:

$$D = \frac{K\lambda}{\cos\theta\sqrt{\beta^2 - \beta_0^2}}$$

where, K = 0.94, λ is the wavelength of incident X-ray radiation (1.5406 $\AA$ for CuKα), β is the intrinsic FWHM of peak, β_0 is the integral peak width resulting from instrumental broadening, and θ is the Bragg's diffraction angle of the XRD peak. The crystallite size is nearly 67 nm.

3.1 SEM Analysis

The surface morphology of activated carbon prepared using alginate with charcoal was obtained using a scanning electron microscope and is shown in Figure 2. The images indicate the surface texture and porosity of the adsorbent. Surface coverage in the form of sphere is evident, showing the presence of inorganic elements, as confirmed by EDAX analysis (Figure 3). These materials are suitable adsorbents owing to their particle morphology. The image exhibits the abundance of roughness and crispy nature, which may be essential to its adsorption ability; additionally, many pores are clearly visible on the surface [17]. In the SEM image, three regions were separately isolated for the characterization of the natural morphology of activated carbon nanoparticles with high surface-to-volume ratios and powerful surfaces that have crystallite sizes of approximately 67. Grain size from SEM analysis is nearly 80 nm, known as activated carbon (AC) nanoparticles. This allowed the impact that increasing surface area which capture of the Ni contaminant. The prepared sample region (a) has an extremely high porosity, negative ions concentration, enhanced discoloring, adsorption, and dispersion invariably For morphological analysis, the surface morphology of the

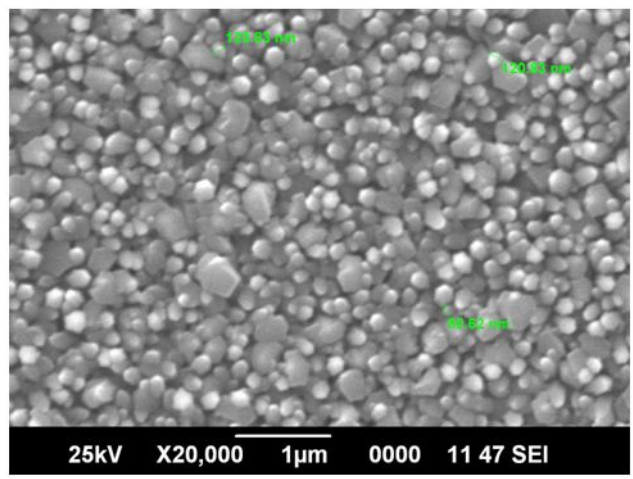

Figure 2. SEM Analysis of activated carbon adsorbent prepared using alginate with charcoal

dried activated carbon with alginate adsorbent was investigated through SEM analysis (Figure. 2). Surface morphology analysis revealed that the activated carbon with the alginate sample exhibits a condensed heterogeneous microstructure and clear surface roughness (Figure. 2 and 3). The surface is extremely dense and compact without any visible porosity. The possible reason is the dramatic shrinking and contraction of activated carbon with alginate beads during evaporative drying and resulting formation of a compact structure with virtually no porous structure (Figure. 2).

3.2 Mechanical properties—Vicker's microhardness

An important use of microhardness study is the possibility of making an indirect estimate of other mechanical characteristics of materials with a specific correlation to their hardness. Transparent and crack-free activated carbon adsorbent beads were used in hardness measurements. The crystal was then subjected to Vicker's microhardness test using HMV. A 2T Shimdazu instrument was used, and Vickers hardness number

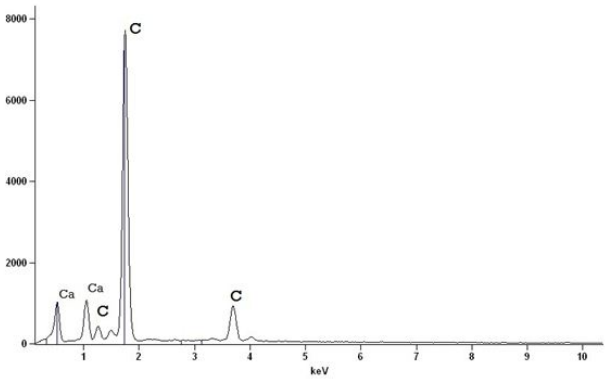

Figure 3. EDAX Analysis of activated carbon adsorbent prepared by alginate with charcoal

Hv was calculated using the relation [18]

$$H_v = 1.8544 \frac{P}{d^2} \left(kg/mm^2 \right)$$

where d is the diagonal length of the indentation and P is the applied load in gram. Variations in Hv at various loads are shown in Table 1 and Figure 4.

Table 1. Microhardness of activated carbon prepared using alginate with charcoal

Load P(gm)	H_x(kg / mm^2)
20	0.0567
40	0.089
60	0.156
80	0.189
100	0.201

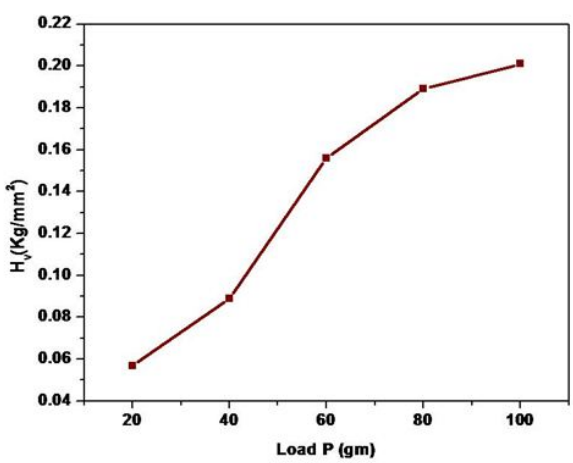

Figure 4. Microhardness analysis of activated carbon prepared using alginate with charcoal

The Vicker's microhardness test revealed that at a low load harness is relatively high and declines at high loads of up to 100 g. The bond energy of the bead may have been caused by the high hardness values at low loads.

3.3 FTIR spectrometry

FTIR analysis was carried out using a NICOLET 185i D1 transmission spectrometer through the KBr pellet technique in a mid IR range of 400–4000 cm^{-1}. The recorded FTIR spectrum of sample crystal is provided in Figure.4. IR absorption measurements show definite bands at 1735, 1590, and 1215 cm^{-1}, which were attributed to the carbon surface structures or conjugated chelated carbonyl and C–O structures. The spectra of the original show absorption bonds at 3737, 2908, 1649, 1017, and 600 cm^{-1} region were detected. The spectra of the original and alkali-treated samples were compared, and the results showed the presence of acidic surface groups. The 1649 absorption band was attributed to carboxylic tautomeric structures, and the 1649 cm^{-1} region spectra showed the considerable overlapping of different absorption bands. These spectra were attributed to quinonic and carboxylate groups. In the 1017 cm^{-1} region, which is the characteristic of O–H bonding vibrations, shows strong reduction after neutralization with alkali was assigned to phenolic groups.

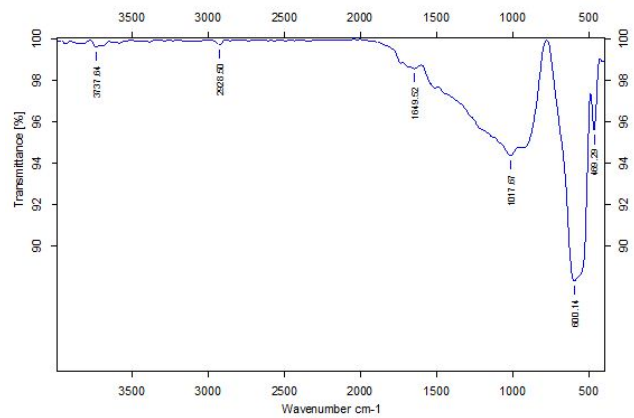

Figure 5. FTIR Analysis of activated carbon prepared using alginate with charcoal

In the analysis of the FTIR vibrational peak of –C(=O)OH group, starting with the OH stretch is preferred. A broad peak found at 3737 cm^{-1} indicates OH stretching. The peak found in the middle of the spectrum around 1649 cm^{-1} was assigned to C=O stretching. The broad envelope between 3737 and 2908 cm^{-1} with multiple peaks confirms the presence of amino group NH2+ stretching. The characteristic vibration of the CO- moiety was found at 600 cm^{-1}. The strong peak determined at 1017 cm^{-1} is due to symmetric NH2+ deformation. The C–C stretching vibrations of the grown crystal appear at 1017 cm^{-1}. The presence of H–Cl group rise to a band at 600 cm^{-1} [19]

4. Adsorption Isotherms and Kinetic Models

4.1 Effect of pH

The pH of a solution is an important parameter for controlling the adsorption process. To investigate the effect of the pH

Table 2. text

Source	Sum of squares	D_f	Mean square	F -Value	P-Value (%)	Comments
Regre ssion	2091.47	9	233.27	186.53	0.07	SD$^{1/4}$ 1.12 %
Lack of pure error	0.08	0	0.08	-	-	R^2 1 / 40.992
Terms	Coefficient	SE Coefficient		t		P -Value (%)
Const ant	71.600	0.659		108.49		0.01
X_1	4.575	0.571		8.000		0.407
X_2	8.375	0.404		20.710		0.0239
X_3	-3.675	0.571		-6.430		0.763
X_{21}	-16.987	0.719		-23.620		0.0166
X_{22}	11.963	0.715		16.630		0.0473
X_{23}	-10.885	0.715		-15.135		0.0626
X_1 X_2	-2.423	0.569		-4.195		2.40
X_1 X_3	1.475	0.981		1.485		23.3
X_2 X_3	-9.975	0.568		-17.435		0.041

of Ni adsorption onto the surface of the activated carbon, we carried out an experiment at a pH range of 2–6. The adsorption rate of Ni increases when the pH of the solution increases from 2 to 6. Notably, at a pH of 6, the amine groups on the activated carbon surfaces are easily protonized. The maximum adsorption capacity occurs at pH 6, followed by a decrease in adsorption, as shown in Figure 6. Thus, the optimum pH for Ni removal is pH 6 [20].

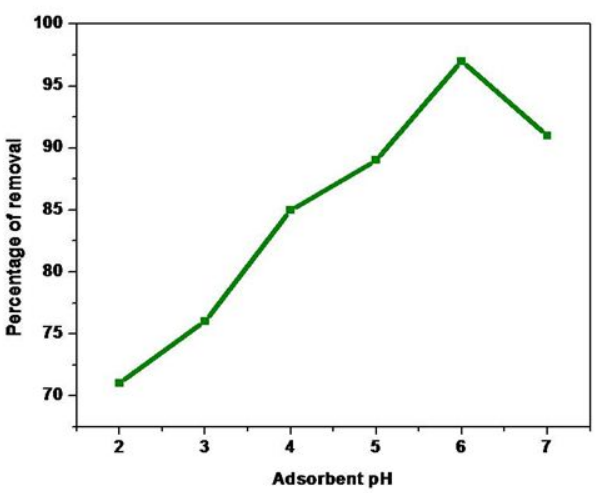

Figure 6. Variation in concentration (ppm) of the adsorbent and percentage of removal

As shown in Table 2, the predicted R2 value (0.992) and adjusted R2 (0.991) values are closely related to each other and are thus in ideal agreement with the quadratic model. This finding suggests that the quadratic polynomial model provides an excellent explanation for the relationship between the process variables and the response. An R2 value of 0.992

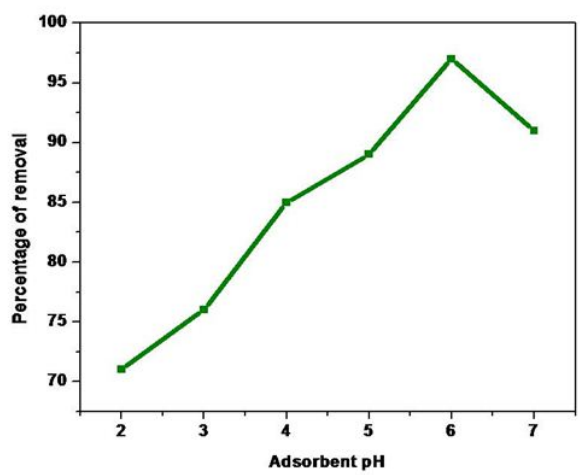

Figure 7. Variation in the pH of adsorbent concentration and percentage of removal

implies that 99.2% of the total variation on Ni adsorption data can be described by the proposed mathematical model and only 0.69% of the total variation cannot be described by the model. According to the ANOVA results (Table 3), the model F-value of 186.53 and p-value of 0.062 % imply that the model is statistically significant, indicating that the proposed mathematical model plotted well to the experimental data on the basis of an insignificant lack-of-t (Table 3). In addition, the significance of each of the linear terms (X1, X2 and X3), the interaction terms (X1X2, X1X3 and X2X3), and the quadratic terms (X12 and X22) on the response were evaluated according to the p-values. The terms with a p-value of less than 5% are significant and hence selected as highly significant model terms.

4.2 Effect of Adsorbent Dosage

The optimum dosage of the adsorbent was determined using experiments from 0.05 gm to 0.5 gm. Figure 8 shows the effect of adsorbent dosage. Rapid increase in adsorption was observed until 0.3 gm possibly because of increase in surface area. A further increase in adsorbent dosage does not result in increase in adsorption, as shown Figure. 7 [21].

4.3 Effect of Contact Time

To establish the appropriate equilibrium time for a Cu adsorption on 1.2 mL of 0.005 Ni SO4+8.8 mL water +100 mg alginate beads, and its adsorption capacities were measured as a function of time. Adsorption rate increases initially but show no notable change after equilibrium. The possible reasons are that the surface area of the adsorbent is occupied and vacant sites for further adsorption are low in number [22]. The absence of change in equilibrium time may not be due to stirring, as shown in Table 3.

4.4 Effect of Agitation Speed and Temperature

Simultaneous observation of speed and temperature are listed in Table 4. Agitation speed on Ni was studied by varying the agitation speed from 100 to 350 for 25 mL of initial concentration 20 ppm solution at pH 6 solution. The optimum agitation speed was calculated from the graph. Adsorption capacity increases with agitation speed possibly because of the diffusion of Ni on the solution [23]. Temperature is an important parameter for controlling adsorption. To study the effect of temperature of adsorption on adsorbent adsorption capacity, we measured adsorbent adsorption capacity as a function of temperature.

Table 2 shows that adsorption increases with temperature owing to the increase in the mobility of metal ions [24].

4.5 Adsorption Kinetics

To investigate the mechanism of adsorption, the pseudo-first-order and pseudo-second- order equation were used in testing the experimental data of initial concentration. The Lagergren [25] rate equation, which is the first rate equation developed for sorption in liquid/solid systems, is based on solid capacity. The pseudo-first-order equation is represented as

$$Log(qe - qt) = logqe - \frac{k_1}{2.303}t$$

where K_2 (g/mg min) is the rate constant of pseudo-second order adsorption. If pseudo-second order kinetics is applicable, the plot t/qt versus t shows a linear relationship and determining any parameter beforehand is not required. Moreover, qe and K_2 can be determined from the slope and intercept of the plot [26], which may involve valency forces through the sharing or exchange of electron between dye anion and adsorption.

The correlation coefficient of the pseudo-second-order kinetic model for the linear plots are more than 0.98. The values of the parameters k_1, k_2 were calculated and are summarized in Table 3. According to the results of correlation coefficient, at initial concentration 50–200 mg/L, the adsorption kinetics follows a pseudo-second order model. At high concentrations (300–500 mg/L), it follows a pseudo-first-order model. This result shows that correlation coefficient is an insufficient criterion for the selection of an adsorption kinetic model [27], derived theoretically that the pseudo-first-order rate coefficient (k_1) is not the intrinsic adsorption rate constant but is a combination of adsorption (ka) and desorption (kd) rate constant $k_1 = k_\alpha C_0 + k_d$. if the adsorption kinetics follows pseudo-first-order, then its rate coefficient is a linear form [28].

Table 4 shows that the relation between k1versus C0 is nonlinear and decreases with increasing C0. Therefore, the initial concentration is between 300 and 500 mg/L, and the adsorption of the prepared solution containing Ni ions does not obey the pseudo-first-order model. The rate coefficient of the pseudo-second-order rate model (k2) is a complex function of the initial concentration of solute (C0). The linear equation of pseudo-first-order kinetic model is represented in the equation

$$ln(qe|qt)^{1/4} lnqe|k_1 t$$

where k_1 is the equilibrium rate constant of pseudo-first-order model (min^{-1}), q_e and q_t refer to the amounts of dye adsorbed on adsorbent (mg g^{-1}) at equilibrium and at time t, respectively. The linear plot of $ln(q_e - q_t)$ versus t is shown in Figure 6b, and Table 4 lists the values of the rate constant k_1, the predicted q_e value, and the correlation coefficient R^2. In general, the best fit can be selected according to the value of the correlation coefficient (R^2) and predicted qe value. In our case, the data in Table 4 show regression coefficient of more than 0.99, but the calculated qe value does not deviate reasonably from the experimental value. The results suggest that our experimental data do not fit well to the pseudo-first-order model, and thus the adsorption process of activated carbon with alginate beads did not obey the pseudo-first-order model. RMSE is a measure how far from the regression line data points

4.6 Catalytic Tests

The catalytic performance of activated carbon with alginate beads prepared through the MCM method was evaluated during the oxidation of benzyl alcohol in the presence of 25% H2O2 as the oxidant. In the catalytic oxidation reaction, benzyl alcohols (5 mmol) and H2O2 (5 mmol) as the oxidant were added with 0.5 g of heterogeneous catalyst (activated carbon with alginate beads), and the contents were heated at 80°C in the presence of acetonitrile (5 mmol) as the solvent for 5 h. Catalytic conversion and product selectivity strongly depend on the particle sizes and surface areas of catalysts, as confirmed by catalytic analysis. The resultant catalysts prepared by two different methods display clear difference in the selective oxidation of benzyl alcohol into benzaldehyde with 100% selectivity.

Table 3. Effect of contact time and its concentration

Time(min)	Absorbance	Concentration	Percentage of removal
0	1.0721	46.3751438	-
10	1.0105	40.506019	12.6
20	0.9488	34.6273664	25.3
40	0.8655	26.690709	42.4
60	0.8504	25.2520112	45.5
80	0.8489	25.1090942	45.85
120	0.8052	20.9454456	54.83
160	0.7783	18.3824674	60.36

Table 4. Kinetic parameters of activated carbon at different initial concentration

Models	Parameters	Activated carbon	Alginate beads
Pseudo-first order kinetic	$q_{e\ exp}$ (mg g-l)	15.35	1.20
	$K_1\left(\mathrm{min}^{-1}\right)$	0.00254	0.00007
	R^2	0.99445	0.99512
	RMSE	0.01663	0.01599
Pseudo-second order kinetic	$q_{\mathrm{e.calc}}\ \left(\mathrm{mgg}^{-1}\right)$	35.95	0.01
	$K_2\left(\ \mathrm{gmg}^{-1}\ \mathrm{min}^{-1}\right)$	0.004	0.095
	R^2	0.99941	0.9981
	RMSE	0.14918	0.1389

4.7 Effects of Surface Area

In general, a high specific surface area has a favorable effect on heterogeneous catalysis. To have an idea of the adsorbance capability of spinel activated carbon with alginate beads, we determined the BET surface area through N2 adsorption/desorption studies. The observed values are provided in Table 4. The surface areas of activated carbon with alginate beads are higher than 29.15 m2/g. In the present study, the surface area parameters of the samples vary with preparation method. Moreover, it is believed that the high surface area of activated carbon with alginate beads could enhance the catalytic activity. The conversion of benzyl alcohol into benzaldehyde for the activated carbon with alginate beads Smoothly proceeds mainly because of the uniform distribution and small particle size of activated carbon with alginate beads as the catalyst.

The oxidation of benzyl alcohol into benzaldehyde was achieved with the 86.25% conversion and 100% selectivity of benzaldehyde and with activated carbon with alginate beads as the catalyst. The conversion rate is higher than that when activated carbon with alginate beads was used at a conversion of 86.54% with 100% selectivity. The observed higher efficiency of activated carbon with alginate beads catalyst in this oxidation reaction can be attributed to the high dispersity and large surface area provides more catalytic active sites for this reaction [44].

4.8 Effect of Catalyst Amount

The influence of catalyst amount on the conversion toward the oxidation of benzyl alcohol into benzaldehyde is shown in Figure 8. The conversion rate gradually increases with the amount of catalyst from 0.1 g to 0.5 g (reaction conditions: catalyst, 0.1– 0.8 g; benzyl alcohol, 5 mmol; acetonitrile, 5 mmol; H2O2, 5 mmol; temperature, 80°C; time, 5 h). After further increase in catalyst amount (0.6–0.8 g), conversion rate and yield remain nearly the same, suggesting that a large amount of catalyst is not needed to improve reaction products [46]. However, with increase in catalyst amount, conversion rate and yield increase up to 0.5 g, and the possible reason is the availability of numerous catalytic active sites in the catalyst [29].

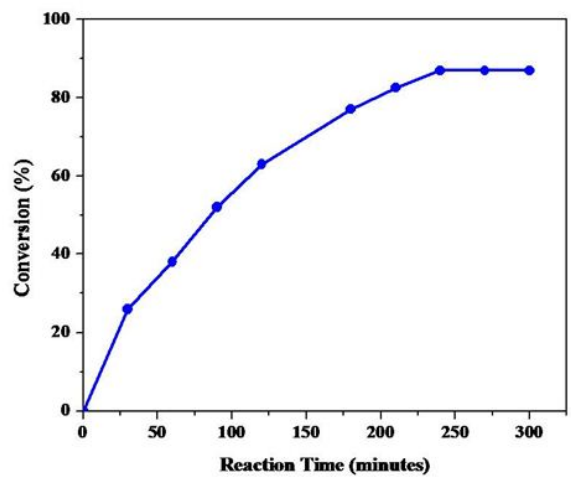

Figure 8. Catalytic reaction time of activated carbon with alginate beads on conversion toward the oxidation of benzyl alcohol into benzaldehyde (reaction conditions: catalyst (0.5 g); benzyl alcohol, 5 mmol; acetonitrile, 5 mmol; H2O2, 5 mmol; temperature, 80°C; time, 5 h).

Table 5. Surface area, conversion, and selectivity percentage for the oxidation of benzyl alcohol into benzaldehyde

Samples	BET surface area $(\mathbf{m}^2/\mathbf{g})$	Conversion (%)	Selectivity (%)
Activated carbon with alginate beads samples	79.86	91.37	100

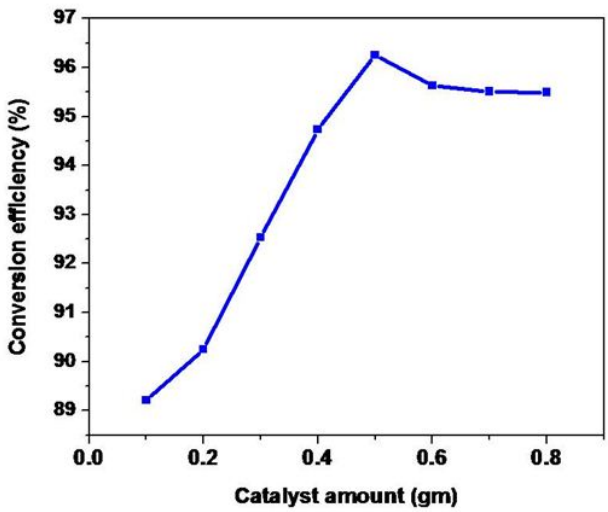

Figure 9. Amount of the spinel catalysts of activated carbon with alginate beads on the conversion toward the oxidation of benzyl alcohol into benzaldehyde (reaction conditions: catalyst (0.1–0.8 g); benzyl alcohol, 5 mmol; acetonitrile, 5 mmol; H2O2, 5 mmol; temperature, 80°C; time, 5 h) [28].

5. Conclusion

Spinel activated carbon was successfully synthesized by using urea as the fuel without any other solvent, surfactant, and catalyst. The MCM method is extremely facile and offers an inexpensive method for preparing nanostructured functional materials compared with the CCM method. Powder XRD, FT-IR, EDX spectra, SAED, HR-SEM, and HR-TEM results showed that the as-prepared samples prepared by MCM were pure phase spinel activated carbon nanospheres and nanoplatelet-like morphology with good crystalline nature without secondary phase impurity. The relatively low Ms (45.16×10^{-3} emu/g) of activated carbon shows that it is a weak ferromagnetic material, and a high Ms (72.42×10^{-3} emu/g) of activated carbon confirms ferromagnetic behavior. The activated carbon shows high conversion (95.25%).

References

[1] Rocher, V., Siaugue, J.M., Cabuil, V. and Bee, A., Removal of organic dyes by magnetic alginate beads. *Water research*, 42(4-5)(2008), 1290-1298.

[2] Pasparakis, G. and Bouropoulos, N., Swelling studies and in vitro release of verapamil from calcium alginate and calcium alginate–chitosan beads. *International journal of pharmaceutics*, 323(1-2)(2006), 34-42.

[3] Ngah, W.W. and Fatinathan, S., Adsorption of Cu (II) ions in aqueous solution using chitosan beads, chitosan–GLA beads and chitosan–alginate beads. *Chemical Engineering Journal*, 143(1-3)(2008), 62-72.

[4] Hari, P.R., Chandy, T. and Sharma, C.P., Chitosan/calcium–alginate beads for oral delivery of insulin. *Journal of Applied Polymer Science*, 59(11)(1996), 1795-1801.

[5] Bajpai, S.K. and Sharma, S., Investigation of swelling/degradation behaviour of alginate beads crosslinked with Ca2+ and Ba2+ ions. *Reactive and Functional Polymers*, 59(2)(2004), 129-140.

[6] Kabbani, A., Karnib, M., Holail, H. and Olama, Z., Heavy metals removal using activated carbon, *silica and silica activated carbon composite,* 2014.

[7] Onundi, Y.B., Mamun, A.A., Al Khatib, M.F. and Ahmed, Y.M., Adsorption of copper, nickel and lead ions from synthetic semiconductor industrial wastewater by palm shell activated carbon. *International Journal of Environmental Science & Technology,* 7(4)(2010), 751-758.

[8] Kayalvizhi, K. and Alhaji, N.M.I., Removal of Copper Using Activated Carbon Adsorbent and Its Antibacterial Antifungal Activity. *European Journal of Medicinal Plants*, (2020), 24-33.

[9] Park, H.G., Kim, T.W., Chae, M.Y. and Yoo, I.K., Activated carbon-containing alginate adsorbent for the simultaneous removal of heavy metals and toxic organics. *Process Biochemistry*, 42(10)(2007), 1371-1377.

[10] Idris, A., Ismail, N.S.M., Hassan, N., Misran, E. and Ngomsik, A.F., Synthesis of magnetic alginate beads based on maghemite nanoparticles for Pb (II) removal in aqueous solution. *Journal of Industrial and Engineering Chemistry*, 18(5)(2012), 1582-1589.

[11] Hassan, A.F., Abdel-Mohsen, A.M. and Fouda, M.M., Comparative study of calcium alginate, activated carbon, and their composite beads on methylene blue adsorption. *Carbohydrate polymers,* 102(2014), 192-198.

[12] Benhouria, A., Islam, M.A., Zaghouane-Boudiaf, H., Boutahala, M. and Hameed, B.H., Calcium alginate–bentonite–activated carbon composite beads as highly effective adsorbent for methylene blue. *Chemical engineering journal*, 270(2015), 621-630.

[13] Ilamathi, R., Nirmala, G.S. and Muruganandam, L., Heavy metals biosorption in liquid solid fluidized bed by immobilized consortia in alginate beads. *International Journal of ChemTech Research*, 6(1)(2014), 652-662.

[14] Zhou, X., Jing, G., Lv, B., Zhou, Z. and Zhu, R., Highly efficient removal of chromium (VI) by Fe/Ni bimetallic

nanoparticles in an ultrasound-assisted system. *Chemosphere*, 160(2016), 332-341.

[15] Aoyagi, R., Sato, R., Terada, A. and Tokuyama, H., Novel composite gel beads for the immobilization of ammonia-oxidizing bacteria: Fabrication, characterization, and biokinetic analysis. *Chemical Engineering Journal*, 342(2018), 260-265.

[16] K Elayakumar, A Manikandan, A Dinesh, K Thanrasu, KK Raja, RT Kumar, Enhanced magnetic property and antibacterial biomedical activity of Ce3+ doped CuFe2O4 spinel nanoparticles synthesized by sol-gel method, *J. Magn. Magn. Mater,* 478(2019), 140-147.

[17] Ayeshamariam, A., Sankaracharyulu, G.V., Kashif, M., Hussain, S., Bououdina, M. and Jayachandran, M., Antibacterial activity studies of Ni and SnO2 loaded Chitosan beads. *In Materials Science Forum*, 832(2015), 110-122.

[18] P Thilagavathi, A Manikandan, S Sujatha, SK Jaganathan, S Arul Antony, Sol–gel synthesis and characterization studies of NiMoO4 nanostructures for photocatalytic degradation of methylene blue dye, *Nanoscience and Nanotechnology Letters*, 8(2016), 438-443.

[19] Bayramoğlu, G. and Arıca, M.Y., Construction a hybrid biosorbent using Scenedesmus quadricauda and Ca-alginate for biosorption of Cu (II), Zn (II) and Ni (II): kinetics and equilibrium studies. *Bioresource technology*, 100(1)(2009), 186-193.

[20] Kinniburgh, D.G., General purpose adsorption isotherms. *Environmental science & technology,* 20(9)(1986), 895-904.

[21] Donohue, M.D. and Aranovich, G.L., Classification of Gibbs adsorption isotherms. *Advances in colloid and interface science*, 76(1998), 137-152.

[22] Begum, K.M.T.M. and Alhaji, N., Adsorption efficiency of sawdust in activated and surface-modified forms-A comparative study. *Chemical Science Transactions*, 2(4)(2013), 1364-1369.

[23] Shafqat, S.S., Khan, A.A., Zafar, M.N., Alhaji, M.H., Sanaullah, K., Shafqat, S.R., Murtaza, S. and Pang, S.C., Development of amino-functionalized silica nanoparticles for efficient and rapid removal of COD from pretreated palm oil effluent. *Journal of Materials Research and Technology*, 8(1)(2019), 385-395.

[24] BEGUM, K.M.T.M. and ALHAJI, N., Spectrophotometric Determination of the Efficiency of Lignocellulosic Sludge-Based Adsorbents in the Removal of Cr (VI) and Ni (II) Ions from Aqueous Solution. *Chemical Science,* 5(3)(2016), 523-540.

[25] Azizian, S., Kinetic models of sorption: a theoretical analysis. *Journal of colloid and Interface Science*, 276(1)(2004), 47-52.

[26] Sirilert, M. and Maikrang, K., Adsorption isotherm of some heavy metals in water on unripe and ripe peel of banana. *Naresuan University Journal: Science and Technology (NUJST)*, 26(1)(2018), 128-141.

[27] Alhaji, N.M.I., Nathiya, D., Kaviyarasu, K., Meshram, M. and Ayeshamariam, A., A comparative study of structural and photocatalytic mechanism of AgGaO2 nanocomposites for equilibrium and kinetics evaluation of adsorption parameters. *Surfaces and Interfaces,* 17(2019), 100375.

⋆⋆⋆⋆⋆⋆⋆⋆⋆

ISSN(P):2319 – 3786
Malaya Journal of Matematik
ISSN(O):2321 – 5666

⋆⋆⋆⋆⋆⋆⋆⋆⋆